Vehicular Communications 50 (2024) 100857

Contents lists available at ScienceDirect

Vehicular Communications

journal homepage: www.elsevier.com/locate/vehcom

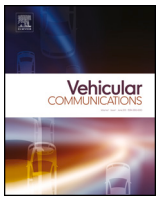

Optimization of electric vehicle charging and scheduling based on VANETs

Tianyu Sun [a], Ben-Guo He [b,*], Junxin Chen [a,*], Haiyan Lu [c], Bo Fang [d], Yicong Zhou [e]

[a] School of Software, Dalian University of Technology, Dalian 116621, China
[b] Key Laboratory of Ministry of Education on Safe Mining of Deep Metal Mines, Northeastern University, Shenyang 110819, China
[c] Faculty of Engineering and Information Technology, University of Technology Sydney, NSW 2007, Australia
[d] School of Computer Science, University of Sydney, NSW 2007, Australia
[e] Department of Computer and Information Science, University of Macau, Macau 999078, China

ARTICLE INFO

Keywords:
Electric vehicle
Charging
Resource allocation

ABSTRACT

Vehicular Ad-hoc Networks (VANETs) provide key support for the achievement of intelligent, safe, and efficient driverless transportation systems through real-time communication between vehicles and vehicles, and vehicles and road infrastructure. This paper investigates a joint optimization problem of electric vehicles (EVs) charging management and resource allocation based on VANETs. EV charging requires significantly more time than refueling conventional vehicles, a key factor behind people's reluctance to transition from internal combustion engine vehicles to EVs. Previous works have primarily concentrated on fully-charged vehicles and random matching, which does not solve the problems of vehicle charging delays and long customer waiting times. Considering these factors, we propose a distributed multi-level charging strategy and level-by-level matching method. Specifically, EVs and passengers are categorized into classes based on battery power and target mileage. Vehicles are then allocated to customers in the same or lower levels. Furthermore, the Attentive Temporal Convolutional Networks-Long Short Term Memory (ATCN-LSTM) model is leveraged to predict historical traffic data, supporting anticipatory decision-making. Subsequently, we develop a hierarchical charging and rebalancing joint optimization framework that incorporates charging facility planning. Experimental results obtained under various model parameters exhibit the method's commendable performance, as evidenced by metrics such as operating cost, system response time, and vehicle utilization.

1. Introduction

With the increasing severity of global climate change and environmental pollution, tailpipe emissions from conventional internal combustion engine vehicles have become a significant international concern. The energy conversion efficiency of EVs can reach 70%-90%, which is 3-4 times higher than that of conventional internal combustion engine vehicles. This allows EVs to travel longer distances using the same amount of energy. Numerous analyses comparing fossil fuel and electrical energy consumption consistently highlight the substantial advantages of transitioning to electric transportation. This shift, particularly in drivetrain electrification, reduces fuel costs and lower emissions per unit of distance traveled [1]. In addition, EVs can be recharged by renewable energy sources (e.g., solar, wind, etc.), further reducing overall energy consumption and carbon emissions and promoting sustainable development. In this context, governments have introduced policy measures to encourage and support the development and promotion of electric vehicle sharing system (EVSS) to minimize the negative impact on the environment and urban traffic [2].

Driven by the low-carbon development policy, the proliferation of EVs and charging facilities is expected to persist. With the rise in the number of EVs, the construction and management of charging infrastructure have emerged as pressing challenges [3]. Traditional approaches to managing charging infrastructure often encounter issues like uneven resource utilization and overloaded stations, impeding the widespread adoption of EVs. Consequently, there's a pressing need to manage EV charging resources and optimize their allocation effectively. Operators must carefully evaluate the economic viability and operational reliability of charging station (CS) construction to ensure seamless integration with existing infrastructures. Additionally, considering the spatial and temporal uncertainties of residents' travel patterns affecting charging demand, constructing stations that prioritize user satisfaction is crucial. Unjustifiable construction impacts operator profits and also leads to charging delays and resource inefficiencies [4]. Thus, striking

* Corresponding authors.
E-mail addresses: hebenguo@mail.neu.edu.cn (B.-G. He), junxinchen@ieee.org (J. Chen).

https://doi.org/10.1016/j.vehcom.2024.100857
Received 3 June 2024; Received in revised form 21 October 2024; Accepted 11 November 2024
Available online 15 November 2024

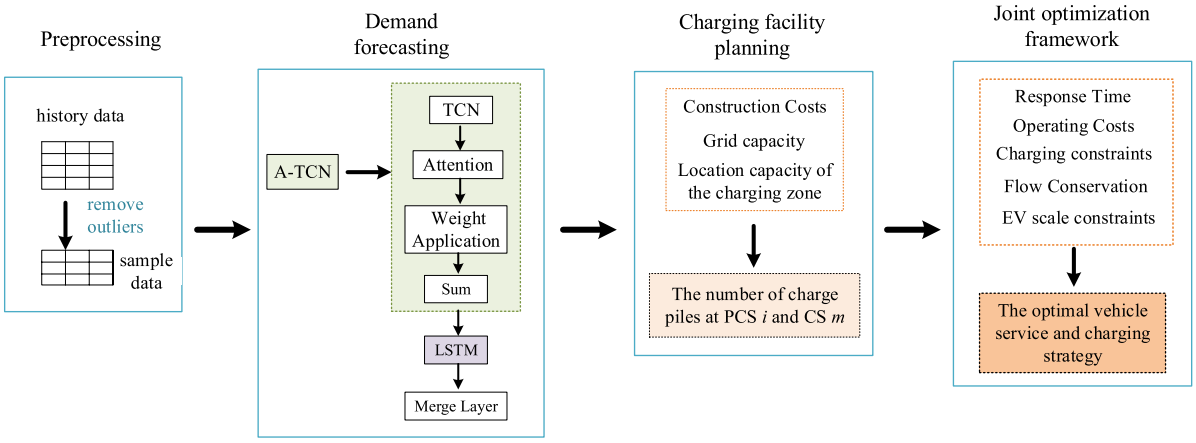

Fig. 1. Framework of the proposed method.

a balance between service quality and construction costs is paramount in the planning phase of EV CSs.

While decision problems related to EVs charging and rebalancing in EVSS have been extensively studied, less attention has been paid to the joint optimization problem for both. In addition, most of the existing studies usually adopt a fully charged strategy, resulting in long charging times. Vehicle congestion and excessively long waiting times may occur at CSs during peak hours, which hinders the widespread adoption of EVs. Existing approaches rely on static or stochastic matching models, making it difficult to respond flexibly to fluctuations in CS demand and dynamic changes in vehicle distribution. Many optimization models favor the operator's interests and neglect user experiences, such as customer waiting time and CS accessibility, which may reduce user satisfaction and affect EV adoption.

In this context, utilizing VANETs technology to optimize EV charging and scheduling problems is a promising solution. VANETs allow real-time communication between vehicles and between vehicles and roadside infrastructures, which strongly supports enhancing the intelligent transportation system (ITS) [5]. Through real-time data exchange and communication, VANETs can facilitate the dynamic optimization of EVSS, balance demand and resources, and minimize system service time. This research aims to explore the potential of VANET-based charging and scheduling optimization for EVs. By combining VANET technology, optimization algorithms, and intelligent decision-making systems, a joint optimization framework of multi-level charging, tiered matching, and vehicle rebalancing is constructed to enhance the operational efficiency, reliability, and scalability of EVSS. We developed a joint optimization framework based on data-based prediction (e.g., Fig. 1). The main contributions of the paper are as follows:

1. We propose a joint optimization model based on queuing theory for multi-level charging and EV rebalancing to enhance travel service efficiency and vehicle availability. Experimental results demonstrate that this model reduces customer waiting times by 5-15 minutes and increases vehicle availability by 15%-30%.
2. Establish an innovative ATCN-LSTM deep reinforcement learning framework for prospective decision-making. Short-term traffic flow prediction using historical data can reduce the prediction error by 4%-14% compared with traditional models.
3. Propose a request-resource allocation method grounded in dynamic planning, which considers the construction of charging piles. In addition, we calculate the number of EV charging piles at each station under local distribution network constraints.

The rest of the paper is organized as follows: related work is discussed in Section 2. Next, Section 3 deals with modeling and problem formulation. A charging pile planning is presented in Section 4. Section 5 is demand forecasting, which contains data processing and forecasting modeling. The experimental simulation is given in Section 6. Finally, conclusions and some future work are drawn in Section 7.

2. Related work

The imbalance between supply and demand for stations and the limited capacity of EV batteries pose significant challenges to operational decisions and CS planning for EVSS. A significant portion of contemporary research tends to segregate the management of EV charging from operational decisions, thus disregarding the mobility and service capabilities of EVs [6].

At the operational level, there are two types of methods in existence: user-based rebalancing schemes and operator-based schemes. The user-based approach leverages pricing incentives to encourage users to drop off vehicles at specific stations, aiming to achieve system equilibrium [7–9]. In the majority of EVSSs, user-based schemes typically serve as a complementary function alongside operator-driven strategies. In operator-driven rebalancing, dedicated operation crews are tasked with relocating idle vehicles from specific stations to those experiencing higher demand. This relocation process aligns with the operator's considerations, including operational costs, benefits, and quality of service, or a balanced trade-off among them. For any objectives, system rebalancing policy can be built on real-time methods like model predictive control [10,11] and steady-state formulations using fluid models [12], queuing algorithms [13,14], network flow methods [15], Markov chain models [16], etc.

At the charge management level, numerous research endeavors have examined various aspects of EV charging, aiming to enhance various performance indicators like charging time and cost through diverse methodologies. Various studies have explored different approaches to charging EV batteries, including grid charging [17], renewable energy charging [18], a hybrid of both [19], battery swapping [20], and wireless charging [21]. Battery swapping and wireless charging often necessitate more expensive infrastructure development. Wireless charging, in particular, tends to be less efficient than wired charging due to energy losses during transfer, leading to slower and less effective charging processes. A queuing network model to estimate the charging demand of EVs and the impact of charging pricing on the CS traffic was proposed in [17]. A multi-class charging management system based on a zone queuing model was proposed in [22], and the [23] developed a CS capacity planning model built upon this framework. In [24], a data-driven EV charging management scheme was proposed to rationalize the allocation of charging piles. Recent advancements have leveraged the connectivity between transportation systems and smart grid infrastructures. Here, EVs requiring charging send requests to roadside units (RSUs) [25,26]. These RSUs then safely guide them to the suitable CS,

Table 1
Comparison of closely related literature.

Reference	Objective	Charging Policy	Rebalancing Process	Prediction Model	Charging Pile
[22]	minimize wait time	multi-level charging	————	————	————
[23]	minimize wait time	multi-level charging	————	————	mathematical model
[24]	maximize operating income	fully charged	————	multi-graph convolutional network	cournot competition model
[30]	minimize the total travel congestion time	fully charged	user-based rebalancing	————	————
[29]	maximize operating income	fully charged	station-based static balancing	graph convolution	————
[31,32]	maximize operating income	fully charged	station-based real-time balancing	————	————
[33]	minimize wait time	multi-level charging	zone-based static balancing	————	————
Our study	maximize operating income and minimize wait time	multi-level charging	station-based real-time balancing	ATCN-LSTM	mathematical model

taking into account the RSU's real-time data and the workload of CS. An efficient method for independent, decentralized vehicle-to-vehicle charging pair allocation was introduced in [27], effectively addressing the challenge of charging information dissemination in VANETs. In [28], they presented a centralized charging management system for mobile EVs, optimizing prospective charging slot reservations to minimize the total service time for energy-demanding vehicles.

However, previous studies have primarily concentrated on EV charging management and operational scheduling separately. Integrating EV scheduling and charging optimization within EVSS remains a largely under explored challenge. In [29], they addressed the problem of vehicle dispatching and recharging decision for an MoD fleet, focusing on the balance of the power grid subject to the V2G operations. A formula integrating a resilience enhancement strategy was proposed in [30]. This formula re-plans routes for low- power EVs to improve system flexibility during emergencies. It also introduces a user balancing principle to account for the self-interested behavior of EV owners, enhancing the formula's applicability. A joint optimization framework based on queuing theory and fluid modeling were given in [31] and extended in [32]. In [33], they addressed a joint problem of rebalancing and charging scheduling of MoD systems from different perspectives. Whereas it was concerned with long distance relocating from vehicle-rich regions to those in need, which cannot cope with supply imbalance between nearby stations. (See Table 1.)

We aim to build a joint optimization framework for hierarchical charging and rebalancing that incorporates charging facility planning, utilizes data-driven predictive models to optimize EV transportation-charging networks in smart cities, and provides support for fleet management, aiming to balance operational costs and quality of service, and improve system responsiveness and vehicle utilization.

3. EV charging and servicing systems

The EV charging process and the service process (including serving customers and vehicle rebalancing, with the rebalancing process viewed as serving virtual customers) are modeled based on queuing theory and fluid models.

3.1. System setup and problem description

Consider a EVSS with N parking-charging stations (PCSs) and M CSs in Fig. 2, each of CS m or PCS i has γ_m and γ_i charging piles, respectively. Including f_m / f_i fast chargers and o_m / o_i ordinary chargers. Denote by μ_f and μ_o the service rate of different chargers. Each of PCS i has p_i parking spaces. Denote by c_f and c_o the cost of charging one level using fast chargers and ordinary chargers, respectively.

The arrivals of customers and customer-carrying vehicles at PCS i are modeled as two Poisson processes [31] with expected rates λ_i^c and λ_i^{vc}, respectively. Denote by b_{ij} and h_{mi} the rate of EVs being relocated from PCS i to j and from CS m to PCS i, respectively. Denote by b_{im} the probability of a vehicle charging from PCS i to CS m. EV battery power at 20%-80% is favorable for battery life [34]. We categorize EVs into K-levels according to their power (as in Fig. 3). k-EVs use graded charging, and 1-EVs use graded charging or full charging. Upon a vehicle arrival at the PCS i, each k-EV, $k \in \{1, \cdots, K-1\}$, will park anywhere in the station until it is assigned to perform the following tasks [35]. i). Join vehicles to serve customers with the current power with probability p_k^{c0}; ii). Recharge its battery from level k to $k+1$ with probability $p_k^{c1}(1-b_{im})$ at PCS i or go CS m with a probability of $p_k^{c1}b_{im}$, where $p_k^{c1} + p_k^{c0} = 1$, then join vehicles to serve customers; iii). To be relocated to PCS j with probability b_{ij}, where $0 \le b_{ij} \le 1$. Let t_{xx} and c_{xx}, respectively, be the travel time and vehicle trip cost (per unit time) between two stations.

In order to achieve refined vehicle-customer matching, both customers and vehicles are graded into K levels based on the trip distance and power, respectively. From the thinning property of Poisson processes, the arrivals of customers and customer-carrying vehicles at level $k \in \{0, \cdots, K\}$ are independent Poisson processes with rates λ_i^{ck} and $\lambda_i^{vc}p_k$. Let $0 \le p_k \le 1$ be the probability that the power of an arriving vehicle belongs to class k. Then $p_K = 0$, as no vehicle will arrive a station with full power after a prior trip, and $\sum_{k=0}^{K-1} p_k = 1$. Similarly, we have $\lambda_i{}^{c0} = 0$, as no customer will request a vehicle to travel no distance, and $\sum_{k=1}^{K} \lambda_i^{ck} = \lambda_i^c$. Assume that each vehicle of class k can serve customers of any sub-level $l \le k$ with probability s_{kl}, where $\sum_{l=1}^{k} s_{kl} = 1, k = 1, \cdots K$. Table 2 summarizes some of the notations used.

3.2. EV service queue

This queueing network has K $M/M/1$ queues corresponding to the K levels of customers services. It is worth noting that EVs can only be assigned to customers of the same level or lower, i.e., k-EVs can only serve customers from level 1 to k. Rebalancing of EVs viewed as the virtual customer service process.

k-EV arrival rate at PCS i is

$$\begin{aligned}&\lambda_i^{vck} = \lambda_i^{vc}(p_k p_k^{c0} + p_{k-1}p_{k-1}^{c1}(1-b_{im})), k = 1 \cdots K-1,\\ &\lambda_i^{vcK} = \lambda_i^{vc}(p_0 p_0^{cK} + p_{K-1}p_{K-1}^{c1}(1-b_{im})).\end{aligned} \tag{1}$$

Arrival rate of vehicles at CS m is

$$\lambda_{im} = \sum_{k=1}^{K-1} \lambda_i^{vck} p_k^{c1} \sum_{m=1}^{M} b_{im}, i = 1, \cdots, N. \tag{2}$$

The rate of EVs at CS m will be relocated to PCS j is

$$\lambda_{mj} = \sum_{j=1}^{N} \sum_{k=1}^{K} \lambda_i{}^{vck} p_k^{c1} b_{im} h_{mj}, m = 1, \cdots, M. \tag{3}$$

The rate of k-EV to be rebalanced from PCS j to i and to serve the customers at PCS i, denote by λ_{ji}^{bk} and λ_i^{ak}, respectively, are

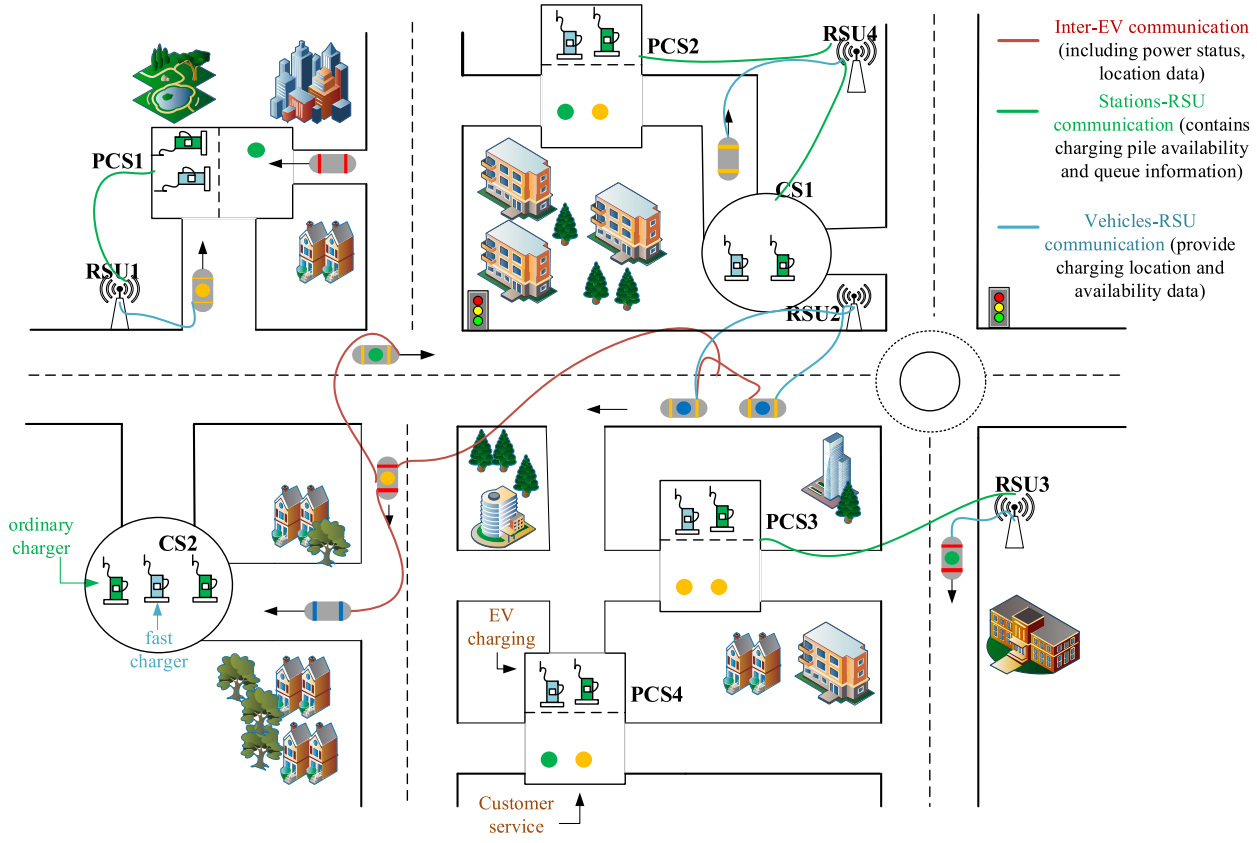

Fig. 2. A schematic diagram of a EVSS with four PCSs, and two CSs. The PCS is divided into customer service and EV charging zones. Different colors represent different level of customers (dots) and EVs (car icons): red for 4-EV, orange for 3-EV, green for 2-EV, blue for 1-EV. Each PCS and CS has two types of charging piles, blue for fast charging piles and green for ordinary charging piles.

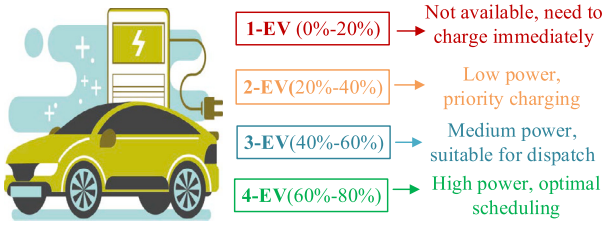

Fig. 3. EVs are categorized into 4 levels based on battery charge.

$$\lambda_{ji}^{bk} = \sum_{i\neq j}^{N} \lambda_j^{vck} b_{ji}, k = 2, \cdots, K,$$
$$\lambda_i^{ak} = \lambda_i^{vck}(1 - b_{ij} - b_{im}), k = 1, \ldots, K. \quad (4)$$

Availability of k-EVs at PCS i is

$$\lambda_i{}^k = \lambda_i^{ak} + \lambda_{ji}^{bk} + \lambda_{mi}^{bk}, k = 1, ..., K. \quad (5)$$

In the same way, we can calculate the rate λ_i^{sk} of k- customers to receive service from EVs as below

$$\lambda_i^{sk} = \sum_{w=k+1}^{K} \left(\lambda_i^{aw} + \lambda_{ji}^{bw} + \lambda_{mi}^{w}\right) p_{wk}^{s}, k = 1, \ldots, K. \quad (6)$$

To ensure that all customers can be served, the stability of the customer queue is

$$\lambda_i^{sk} > \lambda_i^{c(k-1)}, k = 2, \ldots, K. \quad (7)$$

It is also established from queue analysis that the average response time for k-customer in the EVSS is

$$1/(\lambda_i^{sk} - \lambda_i^{c(k-1)}), k = 2, \cdots, K. \quad (8)$$

Table 2
Description of notations.

Symbol	Definition
λ_i^c	arrival rate of customers at PCS i
λ_i^{vc}	arrival rate of customer-carrying EVs at PCS i
λ_i^{ak}	rate of k-EVs that do not participate in rebalancing but directly serve customers at PCS i
λ_{ij}^{b}	rate of rebalancing vehicles from PCS i to PCS j
λ_i^{sk}	rate of class k customer receive service from EVs at PCS i
f_i/o_i	the number of fast /ordinary chargers at PCS i
f_m/o_m	the number of fast / ordinary chargers at CS m
μ_{r_i}	service rate of fully charged EV with depleted battery
p_k	probability that the power of an arriving EV belongs to class k
s_{kl}	rate of k-EV serving l-customers
b_{ij}	rate of rebalancing vehicle from PCS i to PCS j
b_{im}	rate of charging vehicle from PCS i to CS m
p_i^o	rate of EVs at PCS i that do not participate in rebalancing to directly serve customers at PCS i
p_0^{cK}	probability that a battery-depleted EV fully charges
p_k^{c0}	probability that a k-EV serve customers with the current power
p_k^{c1}	probability that a k-EV recharge its battery from class k to $k+1$
c_f/c_o	the cost of charging per level by fast/ordinary chargers
s_f/s_o	the cost of setting up a fast/ordinary chargers
ρ	the service intensity of charging area
P_{free}	the probability that all charging piles are free
γ	the total number of charging piles
L_{EV}	the number of EVs waiting to be charged
$P^{\max}$	the grid's maximum carrying capacity

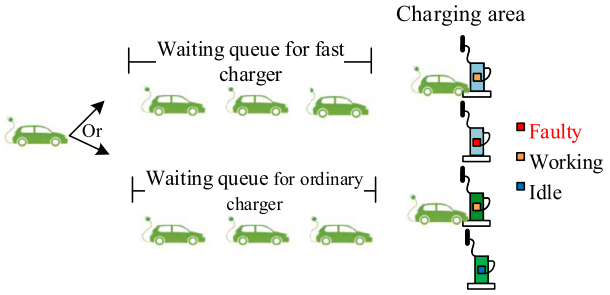

Fig. 4. EV queuing charging process diagram.

To improve the quality of service for customers, the controller of each PCS i must impose an average response time limit. We can express this average response time constraint for the k-customers as

$$1/(\lambda_i^{sk} - \lambda_i^{c(k-1)}) \le T, k = 2, \cdots, K. \tag{9}$$

3.3. EV charging queue

After the EV reaches the charging area, charging service will be provided immediately once an idle charging pile is available; otherwise, the EV will have to wait in line. This process follows the first-come-first-served principle, as shown in Fig. 4.

The charging queue for fast charging piles are modeled as $M/M/f_i$ and $M/M/f_m$, f_i and f_m indicates the number of fast charging piles at PCS i and CS m, respectively. Therefore, the charging demand using fast charger at PCS i and CS m are

$$\lambda_i^f = (\sum_{k=1}^{K-1} \lambda_i^{vc} p_k p_k^{c1} o_i + \lambda_i^{vc} p_0 p_0^{c1} + \lambda_i^{vc} p_0 p_0^{cK}) \alpha_i^f, i = 1, \cdots, N, \tag{10}$$

$$\lambda_m^f = \sum_{i=1}^{N} \sum_{k=1}^{K-1} \lambda_i{}^{vc} p_k p_k^{c1} b_{im}^b \alpha_m^f, m = 1, \cdots, M, \tag{11}$$

where α_i^f and α_i^f are the percentage of EVs charging by fast chargers at PCS i and CS m.

The charging queue for regular chargers is modeled as $M/M/o_i$ and $M/M/o_m$, o_i and o_m indicates the number of ordinary chargers at PCS i and CS m, respectively. The charging demand using regular charger at PCS i and CS m are

$$\lambda_i^o = (\sum_{k=1}^{K-1} \lambda_i^{vc} p_k p_k^{c1} o_i + \lambda_i^{vc} p_0 p_0^{c1} + \lambda_i^{vc} p_0 p_0^{cK}) \alpha_i^o, i = 1, \cdots, N, \tag{12}$$

$$\lambda_m^o = \sum_{i=1}^{N} \sum_{k=1}^{K-1} \lambda_i{}^{vc} p_k p_k^{c1} b_{im} \alpha_m^o, m = 1, \cdots, M, \tag{13}$$

where α_i^o and α_m^o are the percentage of EVs charging by ordinary chargers at PCS i and CS m.

The charging demand for EVs should not exceed the service rate provided by the charging facility. Therefore, Therefore, we can derive stability conditions for charging queues at PCS i are

$$(\sum_{k=1}^{K-1} \lambda_i^{vc} p_k p_k^{c1} (1 - b_{im}) + \lambda_i^{vc} p_0 p_0^{c1}) \alpha_i^f \le o_i \mu_{fi}, i = 1, \cdots, N, \tag{14}$$

$$\lambda_i^{vc} p_0 p_0^{cK} \alpha_i^f \le o_i \mu_{fi}/(K-1), i = 1, \cdots, N, \tag{15}$$

$$(\sum_{k=1}^{K-1} \lambda_i^{vc} p_k p_k^{c1} (1 - b_{im}) + \lambda_i^{vc} p_0 p_0^{c1}) \alpha_i^o \le o_i \mu_{oi}, i = 1, \cdots, N, \tag{16}$$

$$\lambda_i^{vc} p_0 p_0^{cK} \alpha_i^o \le o_i \mu_{oi}/(K-1), i = 1. \cdots, N. \tag{17}$$

Stability conditions for charging queues at CS m are

$$\lambda_m^f \le o_m \mu_{fm}, m = 1, \cdots, M, \tag{18}$$

$$\lambda_m^o \le o_m \mu_{om}, m = 1, \cdots, M. \tag{19}$$

3.4. The joint optimal solution

Given these arguments and variables, the maximum response time T and the rebalancing cost C of the system can be, respectively, given as below:

$$T = \max_{k \in \{1,\ldots,K\}, i \in \{1,\ldots,N\}} 1/(\lambda_i^{sk} - \lambda_i^{ck}), \tag{20}$$

$$C = (\sum_{k=1}^{K-1} t_{im} \lambda_i^{vck} b_{im} + \sum_{m=1}^{M} \sum_{k=1}^{K} t_{mj} \lambda_m^k h_{mj} + \sum_{k=1}^{K} \sum_{i \ne j}^{N} t_{ij} \lambda_i^{vck} b_{ij}) c_{xx} + (\sum_{i=1}^{n} \lambda_i^f + \sum_{m=1}^{M} \lambda_m^f) c_f + (\sum_{i=1}^{n} \lambda_i^o + \sum_{m=1}^{M} \lambda_m^o) c_o, \tag{21}$$

where c_f and c_o are the cost of charging per class by fast and ordinary chargers, respectively.

Given the above stability conditions, the joint optimization problem can be formulated as follows:

$$\min a_1 T + b_1 C, \tag{22a}$$

s.t. (14)-(19)

$$\lambda_i^{sk} - \lambda_i^{c(k-1)} \ge \frac{1}{T}, k = 2, \ldots, K, \tag{22b}$$

$$\lambda_i^c + \sum_{i \ne j}^{N} \lambda_{ij}^b + \sum_{m=1}^{M} \lambda_{im} = \lambda_i^{vc} + \sum_{i \ne j}^{N} \lambda_{ji}^b + \sum_{m=1}^{M} \lambda_{mi}, \tag{22c}$$

$$\sum_{i=1}^{N} \lambda_{im} = \sum_{j=1}^{N} \lambda_{mj}, m = 1, \cdots, M, \tag{22d}$$

where a_1 and b_1 are the weighting coefficient, inequalities (22b) are the stability conditions of the customer queues. Equalities (22c) and (22d) are the stability conditions of traffic flow at PCS i and CS m, respectively.

Based on the above model, we can give the following algorithm for joint optimization (see Algorithm 1).

Algorithm 1 EV scheduling optimization.

Require: l-passenger arrival rate, λ_i^{cl}, k-EV arrival rate, λ_i^{vk}, number of fast /ordinary chargers, f_i, f_m, o_i and o_m
Ensure: Decision variables s_{kl} set, b_{ij} set, b_{im} set, and h_{mj} set, which satisfy constraints and optimization objectives
1: Initialization the parameters
2: Set initial optimal value $Z = +\infty$
3: **for** $l \in [1, K]$, $i \in [1, N]$, $k \in [1, K]$ **do**
4: Initialization $\lambda_i^{vk}, \lambda_i^{cl}, f_i, f_m, o_i$ and o_m, $m = 1, ..., M$
5: Select branch node (i, m, k), according to formula (14)–(19) and (22b)–(22d), $\lambda_i^{vc} p_k (1 - b_{ij} - b_{im}) = \lambda_i^{sk}$, $\sum_{l=1}^{k} s_{kl} = 1$
6: Calculate the $object_{i,m,k}$ according to formula (22a)
7: **if** $object_{i,m,k} \le Z$ **then**
8: (i, m, k) is the current best node, $object_{i,m,k} \to Z$
9: **else if** $object_{i,m,k} > Z$ **then**
10: Branch on node (i, m, k) to generate new sub-level nodes (i_a, m_b, k_c), which satisfy the constraints (14)–(19)and (22b)–(22d).
11: **end if**
12: Calculate the objective value of each new node $object_{i\_a,m\_b,k\_c}$, according to formula (22a)
13: **if** $object_{i\_a,m\_b,k\_c} \le Z$ **then**
14: **continue** repeat the above steps until the sub-nodes at the branch are completely calculated, and $object_{i\_a,m\_b,k\_c} \to Z$
15: **else if** $object_{i\_a,m\_b,k\_c} > Z$ **then**
16: This branch is discarded
17: **end if**
18: **end for**
19: **output** s_{kl} set, b_{ij} set, b_{im} set, h_{mj} set, T and C

4. EV charging infrastructure deployment

Charging piles are classified into fast and normal chargers. This section focuses on the deployment of fast and regular chargers at each PCS and CS.

The basic assumptions of the model as follows:

1. The charging process cannot be interrupted or stopped until the charging task is completed;
2. The charging demand is linearly proportional to its traffic volume.

EVSS charging area service intensity is

$$\rho = \frac{\sum_{i=1}^{N}\sum_{k=1}^{K-1}\lambda_i^{vck}p_k^{c1} + \sum_{i=1}^{N}(K-1)\lambda_i^{vc1}p_0^{cK}}{\sum_{i=1}^{N}(f_i\mu_{fi} + o_i\mu_{oi}) + \sum_{m=1}^{M}(f_m\mu_{fm} + o_m\mu_{om})}. \tag{23}$$

The probability that all charging piles in EVSS are free is

$$P_{free} = [1 + \sum_{d=1}^{\gamma-1}\frac{(\gamma\rho)^d}{d!} + \frac{(\gamma\rho)^\gamma}{\gamma!(1-\rho)}]^{-1}, \tag{24}$$

where γ denotes the total number of charging piles in EMSS, $(\gamma\rho)^d/d!$ indicates the probability that d chargers are serving EVs, and the order of services performed by these chargers does not affect the system's state. $(\gamma\rho)^\gamma/[\gamma!(1-\rho)]$ denotes the probability that all chargers are serving EVs, but EVs are waiting in line.

The number of EVs waiting to be charged is

$$L_{EV} = \frac{P_{free}\rho^2\gamma}{\gamma!(1-\rho)^2}. \tag{25}$$

The construction cost of the charging piles is

$$C_{f+o} = (\sum_{m=1}^{M} f_m + \sum_{i=1}^{N} f_i)s_f + (\sum_{m=1}^{M} o_m + \sum_{i=1}^{N} o_i)s_o. \tag{26}$$

where s_f and s_o denote the cost of setting up a fast charging pile and an ordinary charging pile, respectively.

The charging queue length and charging pile construction cost are taken as optimization objectives, and the charge piles scale optimization model is

$$\min a_2 L_{EV} + b_2 C_{f+o}, \tag{27a}$$

s.t.

$$L_{EV} \le \gamma + H, \tag{27b}$$

$$P_{fast}f_m + P_{ordinary}o_m \le P_m^{\max}, m = 1, \cdots, M, \tag{27c}$$

$$P_{fast}f_i + P_{ordinary}o_i \le P_i^{\max}, i = 1, \cdots, N, \tag{27d}$$

$$f_i, o_i, f_m, o_m \ge 0, \tag{27e}$$

where a_2 and b_2 are the weighting coefficients, the objective is to safeguard charging rates while minimizing costs. Inequality (27b) indicates the charging queue length does not exceed the location capacity of the charging service area, denoted by H the capacity of the charging area. Inequality (27c) and (27d) denote the grid capacity constraints for PCS i and CS m, respectively, and $P^{\max}$ is the grid's maximum carrying capacity (kW). Inequality (27e) is a non-negative constraint. Based on the above factors, we can give the following algorithm for optimization of charging pile size (see Algorithm 2).

Algorithm 2 Optimization process for charging piles size.

1: Initialization the parameters:
l-passenger arrival rate, λ_i^{cl}, k-EV arrival rate, λ_i^{vk}, the capacity of the charging area, H
2: Calculate the intensity of charging service rho and the probability of all charging piles are free P_{free}, according to (23) and (24).
3: **for** $i \in [1, N]$, $m \in [1, M]$ **do**
4: Select a combination of the number of initial fast charging piles and ordinary charging piles (f_i, f_m, o_i, o_m), according to formula (27a)–(27e), and $f_i, f_m, o_i and o_m \in Z_{\ge 0}$
5: Calculate the $object_0$ according to formula (27a)
6: Optimal solutions for different types of charging pile sizes for PCS i and CS m using the cut plane algorithm
7: **end for**
8: **output** f_i, f_m, o_i and o_m

5. Demand forecasting

5.1. Data processing

Our experiment uses the September 2020 Xuancheng city traffic flow dateset. The data includes traffic flow and average speed data for all roadways in the city over a consecutive 30-day period (5-minute counting interval), and floating vehicle trajectory data (10-second sampling interval). In this study, 40W EVs trajectories and traffic flow history data were randomly selected with the time span of 1 month, which specifically contains the elements of vehicle ID, road ID, vehicle location (latitude and longitude), observation time, traveling speed, and travel distance.

Organize dateset into suitable input sequences and corresponding target values. Ensure the data is preprocessed appropriately, including normalization and feature engineering if necessary. Firstly, decontaminating the collected EV historical data removes missing values and outliers (data with travel distance less than 500 m and latitude/longitude not in the intervals 118°28'-119°04' and 30°34'-31°19'). The historical data are then normalized according to equation (28) so that the model inputs become standard data mapped to [-1,1], which reduces computational errors and improves prediction accuracy

$$Data_{input} = \frac{2(Data - Data_{\min})}{Data_{\max} - Data_{\min}} - 1, \tag{28}$$

where $Data$ is the initial traffic data; $Data_{\max}$ and $Data_{\min}$ are the maximum and minimum values in the initial data.

5.2. Prediction model

Utilize a deep structure composed of A-TCN (Attention-based Temporal Convolutional Network) and LSTM to address the traffic flow prediction problem, as illustrated in Fig. 1. This structure is composed of three main components. The first is the A-TCN Module, which incorporates a TCN with an attention mechanism to enhance feature extraction from time series data by focusing on crucial time steps. It uses a convolutional kernel size of 2 with 64 filters and includes four convolutional blocks with dilation rates of 1, 2, 4, and 8. The second component is the LSTM Module, which employs a LSTM network to capture long-term dependencies within the sequential data. Finally, the Fusion Layer combines the outputs of both the A-TCN and LSTM modules, resulting in a more comprehensive and robust feature representation.

Observe the forecasting outcomes, gradually adapt the super-parameters of the algorithm, explore the balance between the volume of input data, the prediction accuracy of the algorithm and the prediction time, determine the optimal super-parameters of the algorithm, form the ATCN-LSTM deep learning network model, and then fit the data using the ATCN-LSTM algorithm. The algorithm evaluates the performance by Mean Absolute Error (MAE), Mean Absolute Percentage Error (MAPE) and Root Mean Squared Error (RMSE).

$$\begin{aligned} MAE &= \frac{1}{N}\sum_{n=1}^{N}|Data_{re} - Data_{pre}|, \\ MAPE &= \frac{1}{N}\sum_{n=1}^{N}|(Data_{re} - Data_{pre})/Data_{re}|, \\ RMSE &= \sqrt{\frac{1}{N}\sum_{n=1}^{N}(Data_{re} - Data_{pre})^2}, \end{aligned} \tag{29}$$

where N denotes the number of samples, $Data_{re}$ is the real value and $Data_{pre}$ is the corresponding predicted value.

The findings presented in Table 3 demonstrate that our proposed approach surpasses the performance of these algorithms in predicting traffic flow within the Xuancheng.

Table 3
Comparison of performance parameters of different prediction models.

Model	MAE	MAPE	RMSE
T-CN	52.4592	0.2082	68.3521
LSTM	66.4825	0.1826	79.8939
GRU	48.7190	0.2351	59.7397
DNN	71.3135	0.2831	84.1592
ATCN-LSTM	42.2869	0.1427	54.0191

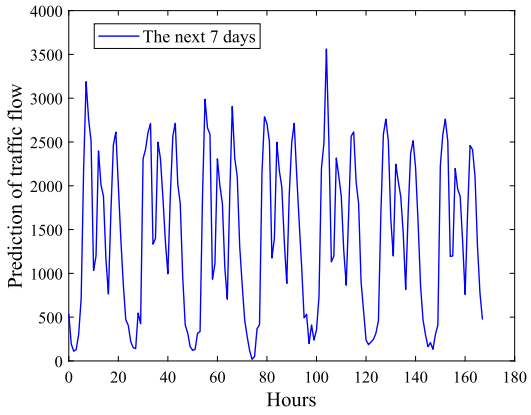

Fig. 5. 7-day prediction of traffic flow.

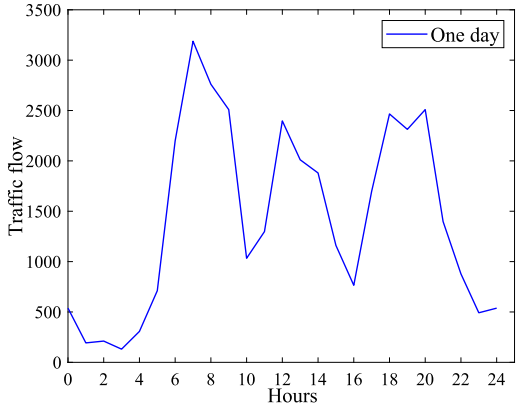

Fig. 6. 1-day prediction of traffic flow.

We employ a dataset spanning 30×24 hours as input features for our time series analysis. The subsequent 7×24 hours are predicted as output. As illustrated in Fig. 5, we note that the traffic flow patterns exhibit remarkable similarity across different days in the dateset. In Fig. 6, we depict the demand for carpooling for passengers over 24 hours. The distribution on one of these days is modeled as having three peaks corresponding to the morning, afternoon, and evening rush hours. In general, we interpret this demand as reflecting the initial ridership of EMSS. To guarantee a superior user experience, our focus lies in evaluating system performance during peak hours.

6. Case studies

This section evaluates the scalability and robustness of the joint optimization framework of rebalancing and multilevel charging strategies through data-driven simulations based on actual traffic data. First, Section 5 describes the processing of the dateset in detail. Then, a comparative analysis of different strategies is presented in Section 6.2, and the superiority of our approach is investigated by analyzing different performance metrics.

Table 4
Location of PCS i and CS m.

PCSi/CSm	Longitude	Latitude
PCS1	118.753632300	30.76398583
PCS2	118.802483800	31.10577010
PCS3	118.704572500	30.97823703
PCS4	118.833528400	31.04456752
PCS5	118.662451700	31.09687117
PCS6	118.647175800	30.95486172
PCS7	118.696475800	30.93594922
PCS8	118.820696600	30.99279910
PCS9	118.652850500	30.90252423
PCS10	118.700519900	31.05570794
PCS11	118.683382500	31.01257589
PCS12	118.817467900	30.91253845
CS1	118.732506000	30.84596527
CS2	118.651853800	31.05027319
CS3	118.742438800	30.93960249
CS4	118.722042600	30.89456922
CS5	118.790152600	30.94637809
CS6	118.732445200	31.11902093

Table 5
Glossary of abbreviations.

Acronyms	Full Name
EV	Electric vehicle
EVSS	Electric vehicle sharing system
VANETs	Vehicular ad-hoc networks
ATCN-LSTM	Attentive temporal convolutional networks-long short term memory
PCS	Parking charging stations
CS	Charging station
ITS	Intelligent transportation system
V2V	Vehicle-to-vehicle
RSU	Road side unit
MAE	Mean absolute error
MAPE	Mean absolute percentage error
RMSE	Root mean squared error
V2X	Vehicle-to-everything

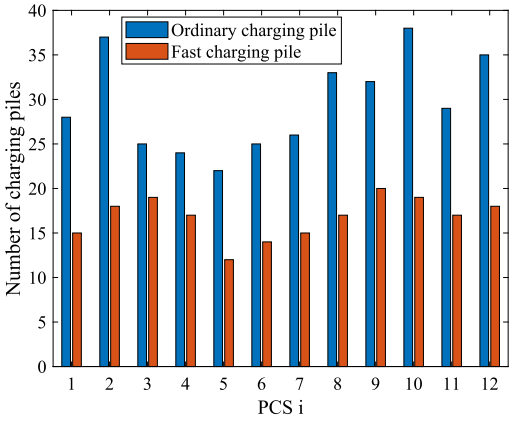

Fig. 7. Planning number of charging piles at PCS i.

6.1. Basic settings

In this section, we verify the method's effectiveness through an example study and evaluate the impact of parameter changes on the system's performance. We have chosen 12 different PCSs and 6 CSs in Xuancheng by performing K-means clustering (see Table 4). Table 5 summarizes several of the acronyms used and their full names. Each PCS i and CS m charging area is fitted with both fast and ordinary charging piles for users to select one. Based on the model simulation analysis, the number of charging piles within PCS i and CS m are shown in Fig. 7 and Fig. 8.

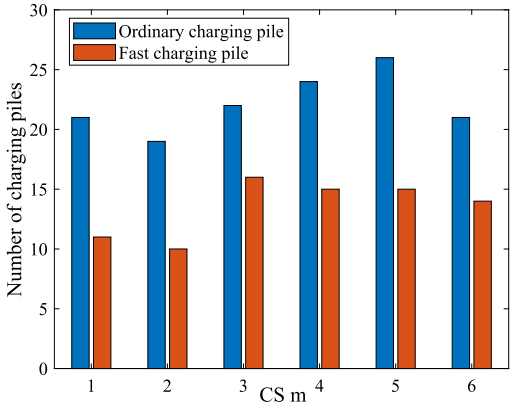

Fig. 8. Planning number of charging piles at CS *m*.

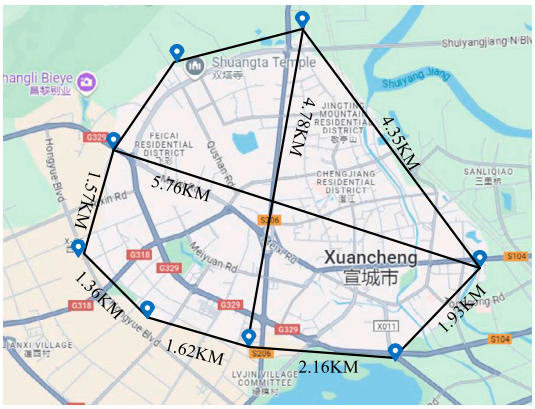

Fig. 10. Straight line distance of Xuancheng transportation routes.

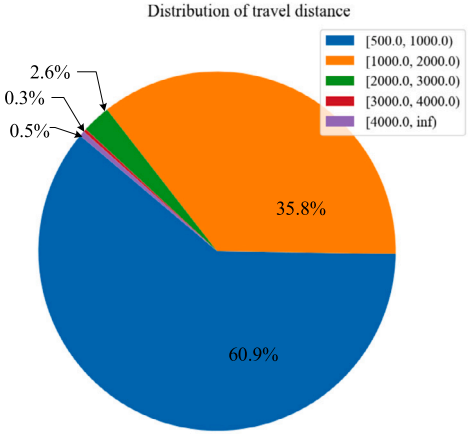

Fig. 9. Distribution ratio of travel distance.

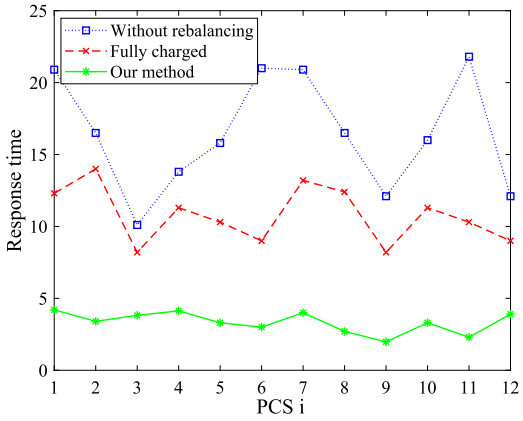

Fig. 11. Vehicle response time at various PCSs.

The charger fleet size optimal model is directly solved using LINGO with computation time of 23 seconds. The fast charging pile is rated at 60 kW, with a construction cost of 80,000 RMB and a charging rate of 1.2 RMB per kWh. In contrast, the regular charging pile operates at 7 kW, with a lower construction cost of 35,000 RMB and a charging rate of 0.7 RMB per kWh. Let the EV fleet size is 2000, and the rebalancing cost is 15RMB/h.

Given an EV with a battery capacity of 60 kWh and a range of 450 km, each charging session allows the vehicle to cover 90 km. As illustrated in Fig. 9 and Fig. 10, depicting the driving mileage distribution of residents and the distances to various locations in Xuancheng, respectively, it becomes apparent that a single charging session is adequate to fulfill residents' daily travel needs.

6.2. Results and analysis

All simulations are performed on a computer with 8192 MB RAM and Intel(R) Core(TM) i7-7500U CPU@2.70 GHz 2.90 GHz Processor. The software used for traffic flow data preprocessing and prediction was IBM SPSS Statistics 26, Python 3.10.4, and PyCharm Community Edition 2022.1; the run time of the prediction model was 27 minutes. LINGO 18.0 was used to solve the joint optimization model, and all the strategies employed were solved in 18 minutes.

Fig. 11 illustrates the system response time at each PCS, representing the waiting duration from when a customer sends an EV request to when they board the EV. The figure demonstrates that the rebalancing approach markedly diminishes the system's response time as the rebalancing method dynamically assigns idle vehicles to areas of higher demand. Furthermore, the graded charging strategy surpasses the traditional complete charging approach in performance. This is because graded charging allows vehicles to return to service quickly after reaching a partial charge, reducing vehicle charging time and idle periods.

Subsequently, the variations of maximum customer wait times, system operating costs, and EV utilization with changes in fleet size are illustrated in Fig. 12. Firstly, there is a decreasing trend in the maximum system response time in Fig. 12(a). This can be attributed to the expansion of fleets, resulting in an increased availability of vehicles to serve more customers simultaneously. However, the improvement tends to flat line after a certain level of fleet size, suggesting that an excessive increase in vehicles does not further significantly reduce waiting times. Secondly, in scenarios where customer demand exceeds the available vehicle capacity, a larger number of vehicles are required for charging or relocation. Conversely, when an ample number of vehicles are available, fewer vehicles necessitate charging and rebalancing, leading to a fluctuating trend in system operating costs, as depicted in Fig. 12(b). Finally, the EV utilization rate under different models shows different trends (see in Fig. 12(c)). With the increase of EV numbers at each station, the model without a rebalancing process has a decreasing trend as the idle EVs at some unpopular stations will accumulate and not be handled in time. For the other two models, more available vehicles serve customers in the early stage and thus increase the overall EV utilization rate. Then, the EV utilization rate starts to decline gradually in the later stage when the number of vehicles continues to grow, but the customer demand remains unchanged. This suggests that while increasing fleet size can improve system performance in the early stages, resource wastage may occur after over-extension. These results indicate that proper fleet sizing and rebalancing strategies are critical for improving EV utilization and reducing system response time. This not only provides valuable guidance for fleet management in ITS, but also offers potential research directions for further optimizing EV scheduling in the future.

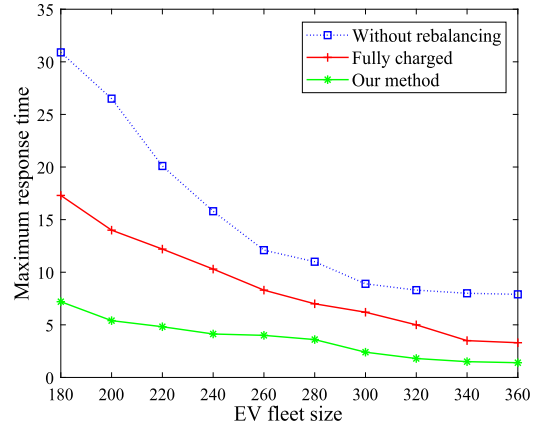

(a)

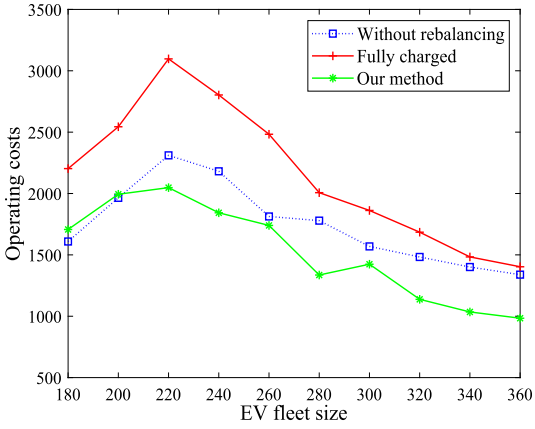

(b)

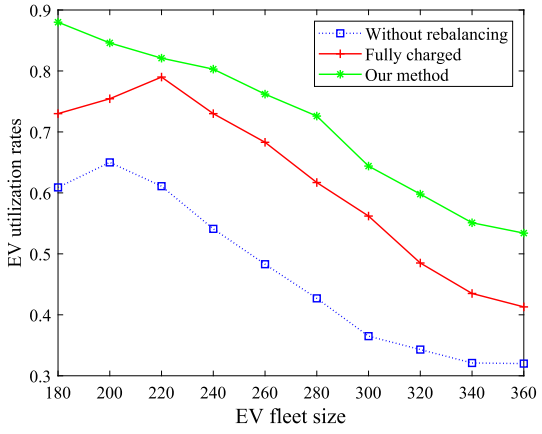

(c)

Fig. 12. Changes in fleet size impact system performance: (a) variation in maximum customer waiting time, (b) changes in system operating costs, and (c) differences in system EV utilization.

We compare the performance of the proposed solution against baseline decision methods under different total customer arrival rates in Fig. 13. It is evident from the figure that our solution outperforms the other three approaches across the entire range. The core of this enhancement lies in the close integration of our proposed graded charging and rebalancing strategies, which can effectively adapt to the system demand under different arrival rates and especially show stronger adaptability and robustness during peak periods. Specifically, the rebalancing approach effectively reduces the system response time and improves

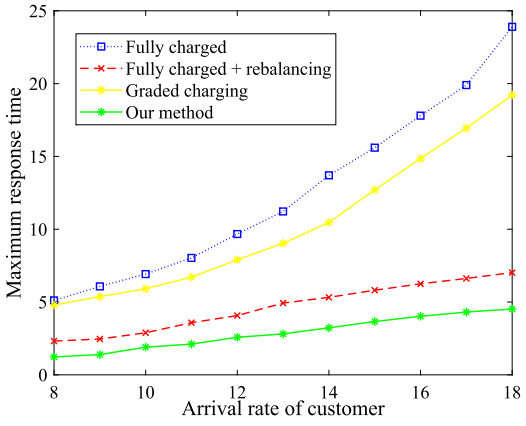

Fig. 13. Performance comparison for different total customer arrival rates.

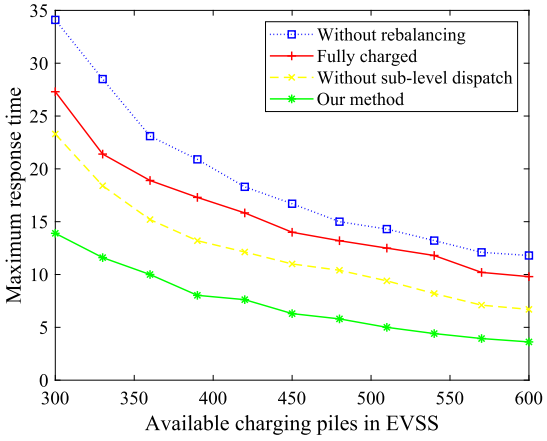

Fig. 14. Impact of number of charging piles on system response time.

the vehicle scheduling efficiency by intelligently allocating resources. In addition, the optimization framework incorporating a hierarchical charging strategy can flexibly respond to fluctuations in customer arrival rates and maintain low charging delays during peak hours.

Due to vandalism or natural damage, certain charging piles will inevitably malfunction resulting in unavailability, so we need to ensure the effectiveness of the model in hard-to-charge situations. Fig. 14 and Fig. 15 depict the robustness performance of our proposed scheme in the case of charging pile reduction. To verify the robustness of the model, we analyze the system response time, vehicle rebalancing cost, and vehicle utilization under different scenarios: without rebalancing, with fully charged vehicles, and with no sub-levels of assigned vehicles, while varying the number of charging piles. As can be seen in Fig. 14 and Fig. 15(b), our proposed solution provides more efficient and reliable customer service. The improvement primarily results from the joint optimization framework, which efficiently allocates available vehicles even as the number of charging piles decreases, preventing a sharp increase in customer waiting times. The rebalancing cost of the system shows an increasing and decreasing trend (see Fig. 15(a)), which is mainly due to the fact that when there are fewer charging facilities, the vehicle needs to go to an area far away from the target station to charge. These results demonstrate the model's robustness in handling damaged or reduced charging piles, ensuring efficient system operation in resource-limited environments.

7. Conclusions

The study proposes a unified framework for hierarchical charging scheduling and rebalancing based on data-driven predictions. This

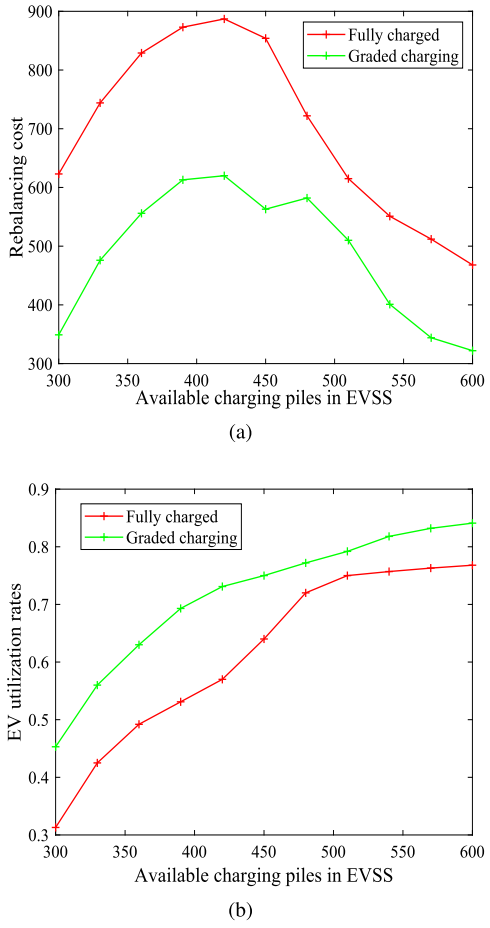

Fig. 15. Superiority of graded charging strategies: (a) changes in system rebalancing costs, (b) changes in EV utilization rates.

framework aims to balance operational costs and service quality while integrating charging infrastructure planning. By leveraging predictive modeling, the framework improves vehicle utilization, reduces maximum response times and associated costs, and enhances overall system resilience. Experimental results show that this approach outperforms traditional methods, demonstrating significant efficiency, cost-effectiveness, and system reliability improvements. In real-world applications, this framework can be deployed to optimize EV charging networks in smart cities, helping operators dynamically manage CSs and allocate resources based on demand forecasts, which also contributes to grid stability and energy optimization. For fleet management, it can improve operational efficiency by ensuring that vehicles are charged at optimal times, reducing downtime and maximizing fleet availability.

However, it is essential to acknowledge some potential limitations and areas for further exploration. The robustness and accuracy of the predictive models under different datasets and real-world conditions deserve further improvement. In addition, fluctuating demand patterns or unexpected disruptions in the charging infrastructure could impact the reliability of the framework. Furthermore, communication challenges, such as latency, network congestion, and packet loss, may affect the exchange of real-time information between vehicles and infrastructure, as well as between vehicles. In order to better service customers, there are some interesting topics worthy of future investigation.

1. Explore prediction models beyond ATCN-LSTM, such as deep reinforcement learning variants or hybrid models, to improve the accuracy and robustness of predictions for different datasets.
2. Investigate the incorporation of vehicle-to-grid technologies to enable bidirectional energy flow between EVs and the power grid. The EV's battery is a decentralized energy storage system that enhances the grid's adaptability to power fluctuations and optimizes grid stability.
3. Extend the optimization framework to integrate advanced V2X communication protocols and emerging technologies like edge computing and 5G to address communication issues, reduce latency, and stabilize data transfers in dynamic vehicular networks. Enhancing the communication layer improves system resilience, ensuring effective operation even with limited or compromised infrastructure.

CRediT authorship contribution statement

Tianyu Sun: Writing – original draft, Validation, Methodology. **Ben-Guo He:** Supervision. **Junxin Chen:** Writing – review & editing, Supervision, Funding acquisition. **Haiyan Lu:** Visualization, Project administration. **Bo Fang:** Resources, Data curation. **Yicong Zhou:** Visualization, Project administration.

Declaration of competing interest

The authors declare that they have no known competing financial interests or personal relationships that could have appeared to influence the work reported in this paper.

Acknowledgements

This work is funded by the National Natural Science Foundation of China (Nos. 62171114, 52222810) and the Fundamental Research Funds for the Central Universities (No. DUT22RC (3)099), and Xiaomi Young Talents Program.

Data availability

Data will be made available on request.

References

[1] G. Wager, J. Whale, T. Braunl, Driving electric vehicles at highway speeds: the effect of higher driving speeds on energy consumption and driving range for electric vehicles in Australia, Renew. Sustain. Energy Rev. 63 (2016) 158–165.
[2] C.L. Canals, L.E. Martinez, G.B. Amante, N. Nieto, Sustainability analysis of the electric vehicle use in Europe for co2 emissions reduction, J. Clean. Prod. 127 (2016) 425–437.
[3] M. Yilmaz, P.T. Krein, Review of the impact of vehicle-to-grid technologies on distribution systems and utility interfaces, IEEE Trans. Power Electron. 28 (2013) 5673–5689.
[4] Z. Danping, L. Juan, C. Yuchun, C. Zhongjian, L. Liping, Research on electric vehicle charging stations planning based on traffic destination heat data and charger usage data, in: IEEE International Conference on Intelligent Transportation Engineering, vol. 3, 2020, pp. 407–410.
[5] H. Abualola, H. Otrok, R. Mizouni, S. Singh, A v2v charging allocation protocol for electric vehicles in vanet, Veh. Commun. 18 (2022) 33.
[6] R. Li, Q. Wu, S. Oren, Distribution locational marginal pricing for optimal electric vehicle charging management, IEEE Trans. Power Syst. 29 (1) (2013) 203–211.
[7] A.D. Febbraro, N. Sacco, M. Saeednia, One-way car-sharing profit maximization by means of user-based vehicle relocation, IEEE Trans. Intell. Transp. Syst. 20 (2) (2019) 628–641.
[8] M. Clemente, M.P. Fanti, G. Iacobellis, M. Nolich, W. Ukovich, A decision support system for user-based vehicle relocation in car sharing systems, IEEE Trans. Syst. Man Cybern. Syst. 28 (2017) 1–14.
[9] D. Jorge, G. Molnar, Dacg Homem, Trip pricing of one-way station-based carsharing networks with zone and time of day price variations, Transp. Res., Part B, Methodol. 81 (2015) 461–482.
[10] A. Carron, F. Seccamonte, C. Ruch, E. Frazzoli, M.N. Zeilinger, Scalable model predictive control for autonomous mobility-on-demand systems, IEEE Trans. Control Syst. Technol. 29 (2) (2021) 635–644.
[11] G.C. Calafiore, C. Bongiorno, A. Rizzo, A robust mpc approach for the rebalancing of mobility on demand systems, Control Eng. Pract. 90 (2019) 169–181.
[12] M. Pavone, S.L. Smith, E. Frazzoli, D. Rus, Load balancing for mobility-on-demand systems, Int. J. Robot. Res. 31 (2012) 839–854.

[13] R. Zhang, M. Pavone, A queueing network approach to the analysis and control of mobility-on-demand systems, in: American Control Conference, vol. 11, 2015, pp. 4702–4709.
[14] R. Zhang, M. Pavone, Control of robotic mobility-on-demand systems: a queueing-theoretical perspective, Int. J. Robot. Res. 35 (2014) 186–203.
[15] F. Rossi, R. Zhang, Y. Hindy, M. Pavone, Routing autonomous vehicles in congested transportation networks: structural properties and coordination algorithms, Auton. Robots 9 (2018) 1–16.
[16] M. Volkov, J. Aslam, D. Rus, Markov-based redistribution policy model for future urban mobility networks 22 (2012) 1906–1911.
[17] H. Liang, I. Sharma, W. Zhuang, K. Bhattacharya, Plug-in electric vehicle charging demand estimation based on queueing network analysis 4 (2014) 1–5.
[18] K. Zhang, Y. Mao, S. Leng, Y. Zhang, S. Gjessing, D.H.K. Tsang, Platoon-based electric vehicles charging with renewable energy supply: a queuing analytical model, in: IEEE International Conference on Communications, vol. 14, 2016, pp. 1–6.
[19] T. Zhang, W. Chen, Z. Han, Z. Cao, Charging scheduling of electric vehicles with local renewable energy under uncertain electric vehicle arrival and grid power price, IEEE Trans. Veh. Technol. 63 (6) (2013) 14–25.
[20] X. Tan, B. Sun, D.H.K. Tsang, Queueing network models for electric vehicle charging station with battery swapping 9 (2014) 1–6.
[21] Y. Shanmugam, R. Narayanamoorthi, P. Vishnuram, M. Bajaj, K.M. AboRas, P. Thakur, Kitmo, A systematic review of dynamic wireless charging system for electric transportation, IEEE Access 10 (2022) 133617–133642.
[22] S. Belakaria, M. Ammous, L. Smith, S. Sorour, R.A. Abdel, Multi-class management with sub-class service for autonomous electric mobility on-demand systems, IEEE Trans. Veh. Technol. 6 (99) (2019) 7155–7159.
[23] M. Asna, H. Shareef, A. Prasanthi, R. Errouissi, A. Wahyudie, A novel multi-level charging strategy for electric vehicles to enhance customer charging experience and station utilization, IEEE Trans. Intell. Transp. Syst. 25 (9) (2024) 11497–11508.
[24] C. Li, Z. Dong, G. Chen, B. Zhou, X. Yu, Data-driven planning of electric vehicle charging infrastructure: a case study of Sydney, Australia, IEEE Trans. Smart Grid 12 (4) (2021) 3289–3304.
[25] B. Aziz, A process algebraic mutation framework with application to a vehicle charging protocol, Veh. Commun. 30 (2021) 1–13.
[26] Al-A. Irfan, T.M. Hussein, Wave 4 v2g: wireless access in vehicular environments for vehicle-to-grid applications, Veh. Commun. 3 (2016) 31–42.
[27] H. Abualola, H. Otrok, R. Mizouni, S. Singh, A v2v charging allocation protocol for electric vehicles in vanet, Veh. Commun. 33 (1) (2022) 1–12.
[28] B.B. Pablo, Lemus C. Leticia, U.A. Luis, A.I. Mónica, A traffic-aware electric vehicle charging management system for smart cities, Veh. Commun. 20 (2019) 100188.
[29] F. Boewing, M. Schiffer, M. Salazar, M. Pavone, A vehicle coordination and charge scheduling algorithm for electric autonomous mobility-on-demand systems 8 (2020) 248–255.
[30] W. Gan, J.F. Wen, M.Y. Yan, Y. Zhou, W. Yao, Enhancing resilience with electric vehicles charging redispatching and vehicle-to-grid in traffic-electric networks, IEEE Trans. Ind. Appl. 60 (1) (2024) 953–965.
[31] G. Guo, T. Xu, Vehicle rebalancing with charging scheduling in one-way car-sharing systems, IEEE Trans. Intell. Transp. Syst. 3 (2020) 1–10.
[32] G. Guo, M. Kang, Rebalancing and charging scheduling with price incentives for car sharing systems, IEEE Trans. Intell. Transp. Syst. 23 (10) (2022) 18592–18602.
[33] N. Yamin, L. Smith, S. Belakaria, S. Sorour, A. Abdel-Rahim, Fleet re-balancing with in-route charging for multi-class autonomous electric mod systems 10 (2020) 1–5.
[34] L. Timilsina, P.R. Badr, P.H. Hoang, G. Ozkan, B. Papari, C.S. Edrington, Battery degradation in electric and hybrid electric vehicles: a survey study, IEEE Access 11 (2023) 42431–42462.
[35] S. Belakaria, M. Ammous, S. Sorour, R.A. Abdel, Fog-based multi-class dispatching and charging for autonomous electric mobility on-demand, IEEE Trans. Intell. Transp. Syst. 21 (2) (2020) 762–776.